**Scheme II**

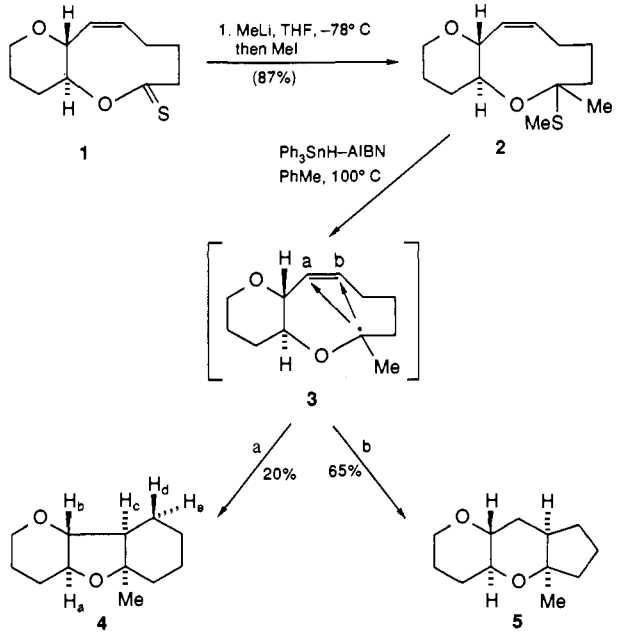


1 2 3 4 5

**Scheme III**

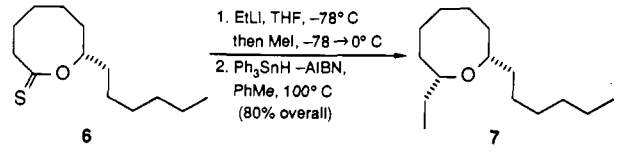


6 7

total synthesis of (±)-lauthisan (**7**),[11] the skeleton of the marine natural product laurencin, from the readily available thionolactone **6**.

The described chemistry opens new routes to mono- and polycyclic ether systems of medium and large sizes from thionolactones. Furthermore, the produced mixed methyl thioketals serve as excellent precursors for free radical generation and, thus, may be found useful in the construction of a variety of complex polycyclic systems via intra- and/or intermolecular trappings. The potential of the present technology in the total synthesis of novel and complex natural products is obvious and is currently under exploration in these laboratories.[12,13]

**Acknowledgment.** We express our many thanks to Mr. John Dykins of this Department for his mass spectroscopic assistance and useful comments. We are also grateful to Professor A. Fukuzawa, Hokkaido University, Japan, and Dr. A. B. Holmes, Cambridge University, UK, for providing us with copies of the NMR, IR, and mass spectra of naturally derived lauthisan. This work was financially supported by the National Institutes of Health, Merck Sharp and Dohme, Hoffmann-La Roche, and Smith Kline and French.

(11) For the naming of this skeleton, see: Blunt, J. M.; Lake, R. J.; Munro, M. H. G.; Yorke, S. C. *Aust. J. Chem.* **1981**, *34*, 2393. For preparation from laurencin, see: Fukuzawa, A.; Masamune, T. *Tetrahedron Lett.* **1981**, *22*, 4081. For a recent total synthesis, see ref 2d.

(12) **Representative Experimental Procedure** (Table I, entry 1). To a stirred solution of caprothionolactone (130 mg, 1.0 mmol) in anhydrous THF (3.0 mL) at −78 °C was added under argon MeLi (0.78 mL of 1.4 M solution in ether, 1.1 mmol). The reaction mixture was stirred at −78 °C for 5 min (TLC monitoring) before quenching with MeI (0.19 mL, 3.0 mmol). The reaction mixture was then allowed to reach ambient temperature with stirring (ca. 1 h). Dilution with ether (50 mL) followed by washing with water (2 × 10 mL), drying ($MgSO_4$), concentration, and flash column chromatography (silica, 10% ether in petroleum ether) gave the corresponding addition product (R = Me, Table I, entry 1, 132 mg, 83% yield).

(13) All new compounds exhibited satisfactory spectral and analytical and/or exact mass data. Yields refer to spectroscopically and chromatographically homogenous materials.

## Bell-Shaped Temperature Dependence in Quenching of Excited $Ru(bpy)_3^{2+}$ by Organic Acceptor

Haeng-Boo Kim, Noboru Kitamura, Yuji Kawanishi, and Shigeo Tazuke*

*Research Laboratory of Resources Utilization*
*Tokyo Institute of Technology, 4259 Nagatsuta*
*Midori-ku, Yokohama 227, Japan*

*Received October 20, 1986*

Electron transfer quenching reactions of excited tris(2,2'-bipyridine)ruthenium(II), $*Ru(bpy)_3^{2+}$, have received special attention as tests of Marcus theory[1] as well as in their application to redox photosensitization.[2] Nevertheless, the mechanism of oxidative quenching of $*Ru(bpy)_3^{2+}$ in acetonitrile, exhibiting negative temperature dependence in endoergic and moderately exoergic regions,[3] is not explicitly understood. We now report the origin of the negative temperature dependence and the reaction mechanism of oxidative quenching of $*Ru(bpy)_3^{2+}$.

The quenching rate constant ($k_q$) at a given temperature was obtained by conventional Stern–Volmer plots based on both the emission intensity and the lifetime of $*Ru(bpy)_3^{2+}$. The effect of diffusion on the observed quenching rate constant was corrected.[4] Typical temperature-dependent data for $k_q$ in acetonitrile are shown in Figure 1. The activation enthalpy ($\Delta H^{\ddagger}$) and entropy ($\Delta S^{\ddagger}$) of quenching were calculated by the Eyring equation,

$$\ln (k_q/T) = \ln (\langle\kappa\rangle k_B K_{12}/h) - \Delta H^{\ddagger}/RT + \Delta S^{\ddagger}/R \quad (1)$$

where $K_{12}$ is the formation constant of an encounter complex.[5] The electronic transmission coefficient $\langle\kappa\rangle$, was assumed to be unity throughout the work. The results are summarized in Table I. The findings are as follows: (a) $\Delta H^{\ddagger}$ is always positive when $\Delta G_{23} < -2$ kcal/mol[6] (Figure 1a, quencher (Q) = 1,4-naphthoquinone). (b) The Eyring plot is "bell shaped" (Figure 1b) when $-2 < \Delta G_{23} < 0$ kcal/mol (Q = duroquinone or *p*-nitrobenzaldehyde). (c) When $\Delta G_{23} > 0$ kcal/mol (Figure 1c, Q = methyl *m*-nitrobenzoate), the temperature dependence of $k_q$ is negative (apparent $\Delta H^{\ddagger} < 0$) in the temperature range examined (−35 to 60 °C). The most striking feature is the finding of a bell-shaped Eyring plot (Figure 1b). This behavior is not due to temperature-dependent solvent viscosity.[4] Furthermore, the temperature

(1) (a) Newton, M. D.; Sutin, N. *Annu. Rev. Phys. Chem.* **1984**, *35*, 437. (b) Sutin, N. *Prog. Inorg. Chem.* **1983**, *30*, 441. (c) Kavarnos, G. J.; Turro, N. J. *Chem. Rev.* **1986**, *86*, 401.

(2) Kalyanasundaram, K. *Coord. Chem. Rev.* **1982**, 46.

(3) (a) Kitamura, N.; Okano, S.; Tazuke, S. *Chem. Phys. Lett.* **1982**, *90*, 13. (b) Tazuke, S.; Kitamura, N. *Pure Appl. Chem.* **1984**, *56*, 1269. (c) Tazuke, S.; Kitamura, N.; Kawanishi, Y. *J. Photochem.* **1985**, *29*, 123.

(4) Observed bimolecular quenching rate constant ($k_q^{obsd}$) was corrected by the equation

$$1/k_q = 1/k_q^{obsd} - 1/k_{12}$$

where $k_{12}$ is the diffusion rate constant in acetonitrile at a given temperature calculated by the Smoluchowski–Stokes–Einstein equation (Smoluchowski, M. *Z. Phys. Chem.* **1917**, *92*, 129):

$$k_{12} = 2RT/3000\,\eta(2 + r_A/r_B + r_B/r_A)$$

$r_A$ and $r_B$ are radii of $*Ru(bpy)_3^{2+}$ (7.1 Å) and a quencher (3.8 Å), respectively. Solvent viscosity ($\eta$) at each temperature was taken from: Janz, G. Z.; Tomkins, R. P.; *Nonaqueous Electrolyte Handbook*; Academic: New York, 1972.

(5) All the quenchers used in this study are neutral molecules, so the $K_{12}$ is given by the following Fuoss equation:

$$K_{12} = 4\pi N r^3/3000,$$

where $r = r_A + r_B$.

(6) $\Delta G_{23}$ was calculated by

$$\Delta G_{23} = E_{1/2}(Ru^{3+/2+}) - E_{1/2}(A^{0/-}) - E_{0\text{-}0} + w_p$$

where $E_{1/2}(Ru^{3+/2+})$ and $E_{1/2}(A^{0/-})$ are the oxidation and reduction potentials of $*Ru(bpy)_3^{2+}$ and an acceptor, respectively (see Table I). $E_{0\text{-}0}$ is the excitation energy of $Ru(bpy)_3^{2+}$, 2.08 eV. $w_p$ is the electrostatic work necessary to separate two product ions to an infinite distance.[1b]

0002-7863/87/1509-2506$01.50/0 

**Table I.** Quenching Rate Constants and Thermodynamics Parameters for Quenching of $*Ru(bpy)_3^{2+}$ by Electron Acceptors in Acetonitrile at 298 K

| electron acceptors | $E_{1/2}$[a] | $kq$, $M^{-1}$ $s^{-1}$ | $\Delta G^{\ddagger}_{23}$, kcal/mol | $\Delta H^{\ddagger}_{23}$, kcal/mol | $\Delta S^{\ddagger}_{23}$, eu[b] | $\Delta G^{\ddagger}_{32}$, kcal/mol | $\Delta H^{\ddagger}_{32}$, kcal/mol | $\Delta S^{\ddagger}_{32}$, eu[b] | $\Delta H^{\ddagger}$, kcal/mol | $\Delta S^{\ddagger}$, eu[b] | $\Delta G_{23}$,[e] kcal/mol | $\Delta H_{23}$,[f] kcal/mol | $\Delta S_{23}$,[f] eu[b] |
|---|---|---|---|---|---|---|---|---|---|---|---|---|---|
| 1,4-naphthoquinone | (−1.08) | $1.3 \times 10^{10}$ | 4.4 | 1.0 | −11.3 | 9.6 | 17.7 | 27.0 | [c] | [c] | −5.28 | −16.7 | −38.3 |
| duroquinone | (−1.22) | $4.7 \times 10^{9}$ | 4.4 | 1.7 | −8.9 | 6.3 | 13.3 | 24.1 | −2.2 | −24.1 | −1.89 | −11.6 | −33.1 |
| *p*-nitrobenzaldehyde | (−1.25) | $2.8 \times 10^{9}$ | 4.6 | 2.4 | −6.2 | 5.7 | 10.7 | 18.2 | −2.6 | −26.2 | −1.16 | −8.3 | −24.4 |
| methyl *m*-nitrobenzoate | (−1.44) | $1.5 \times 10^{7}$ | | | | | | | −4.2[d] | −42.3[d] | 3.13 | −5.9 | −30.6 |

[a] Reduction potentials of electron acceptors (0.1 M tetra-*n*-butylammonium perchlorate used as supporting electrolyte) in volt vs. ferrocenium/ferrocene couple. [b] eu = cal/K mol. [c] The values correspond to $\Delta H^{\ddagger}_{23}$ and $\Delta S^{\ddagger}_{23}$. [d] Could not be resolved to the values corresponding to the $k_{23}$ and $k_{32}$ processes. [e] Oxidation potential of $Ru(bpy)_3^{2+}$ is 0.897 V vs. ferrocenium/ferrocene couple. [f] $\Delta H_{23}$ and $\Delta S_{23}$ were estimated by temperature dependence of $\Delta G_{23}$. See also ref 7.

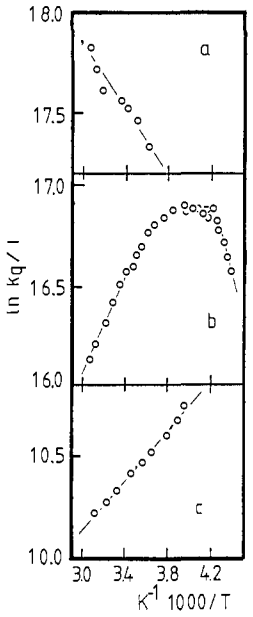


**Figure 1.** Eyring plots for the quenching of $*Ru(bpy)_3^{2+}$ by 1,4-naphthoquinone (a), duroquinone (b), and methyl *m*-nitrobenzoate (c) in acetonitrile.

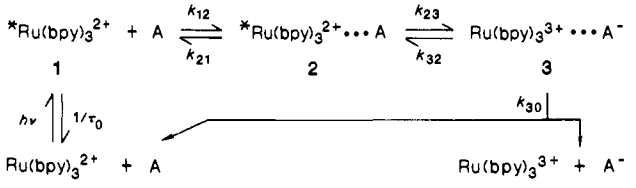


coefficients of the redox potentials for $Ru(bpy)_3^{2+}$ and acceptors are very small[7] so that the characteristic features must be caused by the change in reaction mechanism with temperature.

According to Scheme I, the expression for $k_q$ (eq 2) is simplified to eq 3 and 4, depending on the relative magnitude of $k_{32}$ to $k_{30}$,[8]

$$k_q = K_{12}k_{23}k_{30}/(k_{32} + k_{30}) \quad (2)$$

$$\text{case I} \quad k_{30} \gg k_{32} \quad k_q = K_{12}k_{23} \quad (3)$$

$$\text{case II} \quad k_{30} \ll k_{32} \quad k_q = K_{12}K_{23}k_{30} \quad (4)$$

where $K_{12} = k_{12}/k_{21}$ and $K_{23} = k_{23}/k_{32}$. The apparent activation parameters, $\Delta H^{\ddagger}$ and $\Delta S^{\ddagger}$, are thus expressed as follows.

case I

$$\Delta H^{\ddagger} = \Delta H^{\ddagger}_{23} \quad (5)$$

$$\Delta S^{\ddagger} = \Delta S^{\ddagger}_{23} \quad (6)$$

case II

$$\Delta H^{\ddagger} = \Delta H^{\ddagger}_{23} - \Delta H^{\ddagger}_{32} + \Delta H^{\ddagger}_{30} = \Delta H_{23} + \Delta H^{\ddagger}_{30} \quad (7)$$

$$\Delta S^{\ddagger} = \Delta S^{\ddagger}_{23} - \Delta S^{\ddagger}_{32} + \Delta S^{\ddagger}_{30} = \Delta S_{23} + \Delta S^{\ddagger}_{30} \quad (8)$$

where $\Delta H_{23}$ and $\Delta S_{23}$ represent the reaction enthalpy and entropy of the $k_{23}$ process, respectively. When we compare eq 5 with eq 7, it is apparent that the negative temperature dependence corresponds to case II, $\Delta H_{23}$ being sufficiently negative.[9] Furthermore, by analogy to the Stevens–Ban plot for excimer formation,[10] the appearance of both negative and positive slopes in a bell-shaped Eyring plot is a reflection of the shift of reaction mechanism from case I to case II with increasing temperature. The activation parameters for $k_{23}$, $k_{32}$, and $k_{30}$ can thus be determined by the use of eq 5–8 and independently obtained $\Delta H_{23}$ and $\Delta S_{23}$ (Table I). The observed negative temperature dependence of $k_q$ is in good accordance with the finding $\Delta H_{23} < 0$ and consequently the contribution of $k_{32}$ to the apparent quenching rate constant is proved (case II).

The following discussions on the results in Table I are now warranted:

(i) Although the observed temperature dependence of oxidative quenching rate constant is aberrant (i.e., $\Delta H^{\ddagger} < 0$), the results are perfectly normal when $\Delta H^{\ddagger}_{23}$ and $\Delta H^{\ddagger}_{32}$ are taken into account. $\Delta H^{\ddagger}_{23}$ and $\Delta S^{\ddagger}_{23}$ indicate that electron transfer from $*Ru(bpy)_3^{2+}$ to an electron acceptor proceeds via an enthalpy-controlled reaction path similar to the $*Ru(bpy)_3^{2+}$–electron donor systems.[3,11] As long as the **2** → **3** (see Scheme I) process is concerned, there is no evidence for a mechanistic difference between oxidative and reductive quenching of $*Ru(bpy)_3^{2+}$, since the orbitals involved are different for each mode of quenching.[12]

(ii) The observed large and negative $\Delta S^{\ddagger}$ (−26 to −44 eu) is due to the unfavorable $\Delta S_{23}$ values (−24 to −38 eu). The major contribution to $\Delta S_{23}$ is the change in solvation before and after electron transfer. The calculation of solvation entropy according to the Born model clearly indicates that the **2** → **3** process producing oppositely charged ions (i.e., $Ru(bpy)_3^{3+} + A^-$) is entropically unfavorable while that leading to electrostatically repulsive ions (i.e., $Ru(bpy)_3^{+}$ + donor$^+$) is entropically favored.[13] The situation is inversed for the back electron transfer to the excited reactant pair ($k_{32}$). $k_{32}$ is entropically favorable for ox-

(7) Temperature coefficients of the redox couples, $E_{1/2}(Ru(bpy)_3^{3+/2+})$ and $E_{1/2}(A^{0/-})$, are estimated to be ~0.4 mV/K and ~−1 mV/K (averaged for all acceptors used), respectively, by cyclic voltammetry using nonisothermal cell configuration. (See also: Yee, E. L.; Cave, R. J.; Guyen, K. J.; Tyma, P. D.; Weaver, M. J. *J. Am. Chem. Soc.* **1979**, 101, 1131. Hupp, J. T.; Weaver, M. J. *Inorg. Chem.* **1984**, *23*, 3639. Variation of the dielectric constant of the medium (Burflinger, A. *Ber Bunsenges. Phys. Chem.* **1980**, *84*, 653) and, thus, that of $w_p$ with temperature were corrected for the calculation of $\Delta G_{23}$.

(8) Bock, C. R.; Connor, J. A.; Guiterrez, A. R.; Meyer, T. J.; Whitten, D. G.; Sullivan, B. P.; Nagle, J. K. J. Am Chem. Soc. 1979, 101, 4815.

(9) Sutin, N. *J. Photochem.* **1979**, *10*, 19.

(10) Birks, J. B. *Photophysics of Aromatic Molecules*; Wiley-Interscience: London, 1970.

(11) Baggott, J. E. *J. Phys. Chem.* **1983**, *87*, 5223.

(12) The $d\pi^*$ and $t_{2g}$ oribtals of $*Ru(bpy)_3^{2+}$ are involved in the quenching by electron acceptors and donors, respectively.

(13) Shmits, J. E. S.; van der Linden, J. G. M. *Inorg. Chem.* **1984**, *23*, 3298.

idative quenching of $*Ru(bpy)_3^{2+}$, rendering the case II mechanism.

(iii) The activation enthalpy and entropy calculated from the Marcus expressions using $\Delta H_{23}$ and $\Delta S_{23}$[14] run parallel to the observed ones.[15] Qualitatively, both the **2** → **3** and **3** → **2** processes are explainable within the framework of Marcus theory.

(14) (a) Brown, G. M.; Sutin, N. *J. Am. Chem. soc.* **1979**, *101*, 883. (b) Sutin, N. *Tunneling in Biological Systems*; Chance, B., Ed.; Academic: New York, 1979.

(15) Kim, H.-B.; Kitamura, N.; Tazuke, S. unpublished results.

## Multiple Bonds between Transition Metals and Main Group Elements: "Naked" Lead in a Planar Environment[1]

Heinz-Josef Kneuper, Eberhardt Herdtweck, and Wolfgang A. Herrmann*

*Technische Universität München*
*Lehrstuhl I für Anorganische Chemie*
*D-8046 Garching, West Germany*
*Received November 7, 1986*

Bare main group elements, surrounded by transition-metal fragments via multiple bonds, are no longer curiosities in organometallic chemistry since several synthetic routes have lately been developed for this class of compounds.[2] To name just two important examples, the unique cumulene-type germanium,[3] tin,[4] and lead compounds[5] of type A are made from monogermane ($GeH_4$), tin dichloride, and lead dichloride, respectively, while the bent tellurium species B results from treatment of elemental tellurium or tellurium hydride ($TeH_2$) with a closely related organometallic precursor.[6]

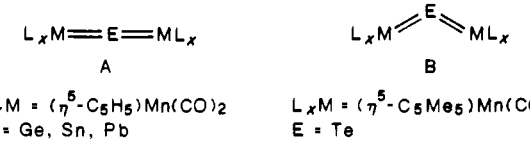


The central main group elements of such compounds are sterically exposed, thus being centers of high reactivity.[2] We have now achieved the first example of trigonal-planar coordination of the element lead. At this occasion, we demonstrate a further stepwise synthesis of oligonuclear organometallics centering around unsubstituted main group elements.

Treatment of the heterocumulene-type MnPbMn precursor species **1** with an excess of the solvent-stabilized fragment ($\eta^5$-$C_5H_4CH_3)Mn(CO)_2$ (as THF adduct **2**) at room temperature yields a reaction mixture from which the novel $Mn_3Pb$ compound **3** can be isolated by column chromatography (silica, +15 °C) in ca. 50% yield (Scheme I). This complex crystallizes in black crystals that are not only extremely air-sensitive but can be handled at room temperature only for a brief period of time. Elemental analysis and IR and $^1H$ NMR spectra established the net formula $[(\eta^5\text{-}C_5H_4CH_3)Mn(CO)_2]_3Pb$,[7] while a single-crystal X-ray diffraction study at −80 °C confirmed the suggested structure, revealing a strictly planar $Mn_3Pb$ core (Figure 1).[8]

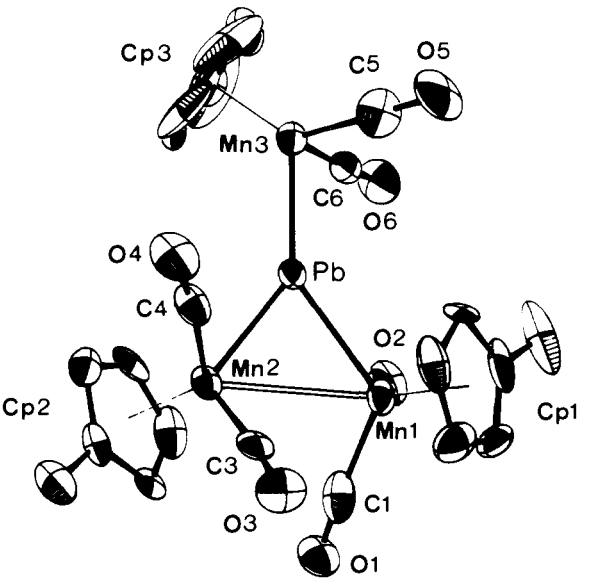


**Figure 1.** ORTEP representation of the $Mn_3Pb$ compound **3** (−80 °C). Selected bond lengths [pm] and angles [deg]: Mn(1)–Pb 262.0 (1), Mn(2)–Pb 261.1 (1), Mn(3)–Pb 249.0 (1), Mn(1)–Mn(2) 311.0 (1); Mn(1)–Pb–Mn(2) 72.97 (4), Mn(1)–Pb–Mn(3) 143.56 (4), Mn(2)–Pb–Mn(3) 143.41 (4).

**Scheme I**

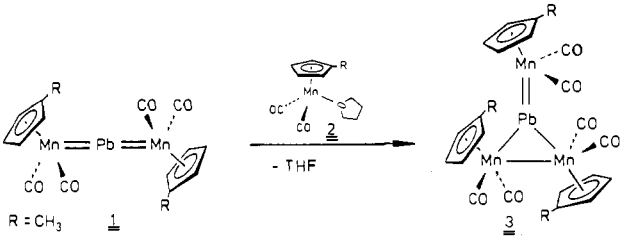


The sum of angles around lead amounts of 359.9 (1)°. There are two different types of coordinated ($\eta^5$-$C_5H_4CH_3)Mn(CO)_2$ fragments: the distances Mn(1)–Pb and Mn(2)–Pb were recorded to be 262.0 (1) and 261.1 (1) pm, respectively, thus being in excellent agreement with single bonds that may be estimated at ca. 261 pm from the elements' covalent radii.[4] To our knowledge, these are the first structurally documented manganese-to-lead single bonds. The Mn(3) fragment, however, is much closer to the central lead atom, with the recorded distance of 249.0 (1) pm being consistent with the formal assignment of a double bond as it results from the EAN rule. Slightly shorter MnPb distances were found in the linear $Mn_2Pb$ skeleton of the precursor species **1** ($d$(MnPb) = 246.3 (1) pm).[5] A bond length of 311.0 (1) pm between the manganese atoms Mn(1) and Mn(2) suggests metal–metal interaction.[9] The structural data hence support the

(1) Communication 37 of the series *Multiple Bonds between Transition Metals and Main Group Elements*. This work is being supported by the German Federal Ministry of Research (BMFT), Bonn. Preceeding paper: Herrmann, W. A.; Weichselbaumer, G.; Kneuper, H.-J. *J. Organomet. Chem.* **1987**, *319*, C21.

(2) For a recent review, see: Herrmann, W. A. *Angew. Chem.* **1986**, *98*, 57; *Angew. Chem., Int. Ed. Engl.* **1986**, *25*, 56.

(3) Gäde, W.; Weiss, E. *J. Organomet. Chem.* **1981**, *213*, 451.

(4) Kneuper, H.-J. Ph.D. Thesis, Technische Universität München, 1986.

(5) Herrmann, W. A.; Kneuper, H.-J.; Herdtweck, E. *Angew. Chem.* **1985**, *97*, 1060; *Angew. Chem., Int. Ed. Engl.* **1985**, *24*, 1062.

(6) Hecht, Ch.; Ziegler, M. L.; Balbach, B.; Herrmann, W. A. *J. Chem. Soc., Chem. Commun.* **1984**, 686.

(7) Spectroscopic data: IR ($\nu$CO) 1962 m, 1943 m, 1933 vs, 1923 s, 1905 w, 1896 w, 1884 m (*n*-hexane), 1958 s, 1923 vs, 1920 sh, 1891 sh, 1879 m ($Et_2O$) cm$^{-1}$; $^1H$ NMR (270 MHz, $C_6D_5CD_3$, 25 °C) $\delta$ 4.61 (m, 2 H), 4.26 (m, 2 H), 3.97 (m, 4 H), 3.88 (m, 4 H), 2.04 (s, 6 H), 1.69 (s, 3 H). Anal. Calcd for $C_{24}H_{21}Mn_3O_6Pb_3$ (777.33): C, 37.07; H, 2.70; Mn, 21.19; Pb, 26.64. Found: C, 36.78; H, 2.74; Mn, 21.30; Pb, 27.01.

(8) Black, triclinic columns grown from dichloromethane/*n*-hexane at −30 °C, space group $P\bar{1}$ (IT: No. 2), $a$ = 940.3 (1) pm, $b$ = 1177.8 (2) pm, $c$ = 1342.1 (2) pm, $\alpha$ = 67.56 (2)°, $\beta$ = 78.86 (1)°, $\gamma$ = 63.96 (1)°, $V$ = 1234 × 10$^6$ pm$^3$, $Z$ = 2, $F$(000) = 740, $d$(calcd) = 2.093 g·cm$^{-3}$, $\mu$ = 83.32 cm$^{-1}$, $T$ = −80 ± 1 °C, CAD4 (Enraf-Nonius) Mo K$\alpha$ radiation, graphite monochromator, $\omega$-scan, 2.0° < $\theta$ < 25°, $h$(−11/11), $k$(0/6), $l$(−15/15), $t$(max) = 45 s, number of recorded data 3009, independent reflections 2783, of which 153 unobserved reflections with $I < 1\sigma(I)$ were excluded from refinement. The structure was solved by Patterson methods and difference Fourier syntheses. All non-hydrogen atoms were refined anisotropically, and hydrogen atoms were calculated from ideal positions and included in structure factor calculations: 307 parameter full matrix, $R$ = 0.041, $R_w$ = 0.050; GOF = 3.273. For all calculations the program system STRUX-II was employed. Further details of the crystal structure determination can be obtained from the Fachinformationszentrum Energie Physik Mathematik, D-7514 Eggenstein-Leopoldshafen 2, Germany, by quoting the depository number CSD 52281, the names of the authors, and the journal citation.

(9) Bernal, I.; Creswick, M.; Herrmann, W. A. *Z. Naturforsch., B: Anorg. Chem., Org. Chem.* **1979**, *34B*, 1345.

0002-7863/87/1509-2508$01.50/0 